Chem Soc Rev

Two-photon polymerization microfabrication of hydrogels: an advanced 3D printing technology for tissue engineering and drug delivery

Journal:	*Chemical Society Reviews*
Manuscript ID:	CS-TRV-04-2015-000278
Article Type:	Tutorial Review
Date Submitted by the Author:	03-Apr-2015
Complete List of Authors:	Xing, Jinfeng; Tianjin University, Zheng, Mei-Ling; Technical Institute of Physics and Chemistry, Chinese Academy of Sciences, Lab of Organic NanoPhotonics Duan, Xuan-Ming; Tehcnical Institute of Physics and Chemistry, Chinese Academy of Sciences, Lab Organic NanoPhotonics

Journal Name

RSCPublishing

ARTICLE

Two-photon polymerization microfabrication of hydrogels: an advanced 3D printing technology for tissue engineering and drug delivery

Jin-Feng Xing[a*], Mei-Ling Zheng[b], Xuan-Ming Duan[bc*]

Cite this: DOI: 10.1039/x0xx00000x

Received ooth January 2012,
Accepted ooth January 2012

DOI: 10.1039/x0xx00000x

www.rsc.org/

3D printing technology has attracted much attention due to its high potential in scientific and industrial applications. As an outstanding 3D printing technology, two-photon polymerization (TPP) microfabrication has been applied in the fields of micro/nanophotonics, micro-electromechanical systems, microfluidics, biomedical implants and microdevices. In particular, TPP microfabrication is very useful in tissue engineering and drug delivery due to its powerful fabrication capability for precise microstructures with high spatial resolution on both the microscopic and the nanometric scale. The design and fabrication of 3D hydrogels widely used in tissue engineering and drug delivery has been an important research area of TPP microfabrication. The resolution is a key parameter for 3D hydrogels to simulate the native 3D environment in which the cells reside and the drug is controlled to release with optimal temporal and spatial distribution *in vitro* and *in vivo*. The resolution of 3D hydrogels largely depends on the efficiency of TPP initiators. In this paper, we will review the widely used photoresists, the development of TPP photoinitiators, the strategies for improving the resolution and the microfabrication of 3D hydrogels.

Keywords: 3D printing technology, two-photon polymerization microfabrication, 3D hydrogels, resolution, TPP initiator.

A. Introduction

The invention of typography by Sheng Bi in the 10th century, woodblock printing by Zhen Wang in the 13th century in China, and the subsequent development of the industrial-scale printing press in the 15th century, facilitated rapid reproduction of text and images and the dissemination of information. Printing has revolutionarily influenced on society, education, politics, religion and language across the globe. In the past few decades, printing technology has evolved from two-dimensional (2D) printing to 3D printing as an additive process in which successive layers of material are combined to form 3D shapes. At present, 3D printing technology has been received increasing attention and applied in the fields, including large-scale industrial prototyping, the production of tissue scaffolds, biomimetic microvascular systems, the manufacture of bespoke electronic and pneumatic devices.[1] 3D printing begins with a 3D model of the object, which is then digitized and sliced into model layers with special software. The 3D printing system then prints 2D layers into a 3D build by adding each new layer on top of the prior layer. These layers are combined to form the final product.[2]

3D printing was first described in 1986 by Charles W. Hull. In his method named sterolithography (SL), thin layers of a material that can be cured with ultraviolet light were sequentially printed to form a solid 3D structure. For common SL of single-photon polymerization (SPP), an initiator in photopolymerizable resin (photoresist) mainly composed of monomer and oligomer absorbs one UV photon with a short wavelength through a linear absorption to initiate polymerization.[1] Due to the poor penetrating ability, the UV light is absorbed by the photoresist within the first few micrometers. Although classic 3D prototyping techniques such as UV laser microstereolithography, 3D inkjet printing and laser sintering can also produce fully 3D structures, they cannot provide resolution better than a few microns. On the other hand, lithographic techniques with superior resolution, such as electron beam or atomic force lithography, cannot produce

anything more complicated than high-aspect ratio 2D structures, and the fabrication throughput is relatively very low.[3]

Unlike other 3D printing technologies, two-photon polymerization (TPP) microfabrication (TPPM) induced by a near-infrared femtosecond laser can fabricate arbitrary and ultraprecise 3D microstructures with high resolution not only on the microscopic scale but also on the nanoscale.[4, 5] So far, femtosecond laser-induced TPPM has been widely applied in fields such as micro/nanophotonics,[6, 7] micro-electromechanical systems (MEMS),[8, 9] microfluidics,[10] biomedical implants and microdevices.[11, 12] TPP process is initiated by three-order nonlinear absorption within the focal region. 3D structures can be fabricated by moving the focused beam in photoresist according to computer-designed 3D route with the resolution beyond the optical diffraction limit.[13, 14] Many typical and useful microstructures such as photonic crystals,[15] mechanical devices[9] and 3D hydrogels[16] have been fabricated by TPP microfabrication. Particularly, 3D hydrogels have been achieved ongoing intense research activity due to their promising biomedical applications in tissue engineering and drug delivery.[17-19] The resolution is crucial for 3D hydrogels to simulate the native 3D environment in which cells reside and drug is controlled to release with optimal temporal and spatial distribution *in vitro* and *in vivo*.[20] Many strategies have been developed to improve the resolution of TPP to be less than 100 nm.[21-25] In TPP, the spatial resolution is dominantly determined by laser power and exposure time,[22] which largely depends on the efficiency of TPP initiators. In this review, we will review the widely used photoresists, the development of TPP photoinitiators, the strategies for improving the resolution and several microstructures of 3D hydrogels.

B. The principles of two-photon absorption (TPA) and TPP

In this part, we will concisely introduce the principles of TPA and TPP. If readers want to know more details, they can get them from the typical references.[26-29] TPA is a three-order nonlinear optical phenomenon predicted in theory by Göppert-Mayer in the 1930s and demonstrated in experiment by Kaiser in 1961 after the invention of the laser. Laser with high intensity of pulse peak provides a powerful tool to characterize TPA, in which one molecule simultaneously absorbs two photons to reach to the excited state from the ground state. The degree of TPA scales with the square of incident light intensity and the maximum absorption occurs at the focal point of light. The basic principle of TPA is shown in Fig. 1.[30] A molecule is exited from the ground state (*g*) to an excited state (*f*) located at energy E_f (above the *g* state) by absorbing two photons (vertical solid arrows). The photons can have the same energy, E_1 (degenerate case, $E_f = 2E_1$), or different energies, E_1 and E_2 (nondegenerate case, $E_f = E_1+E_2$). After excitation, the system relaxes quickly to state denoted as *r*, the lowest vibronic level of the lowest-energy excited state by internal conversion or vibrational relaxation (dashed arrow). The system finally returns to the ground state by radiative or nonradiative pathways (bold dashed arrow).

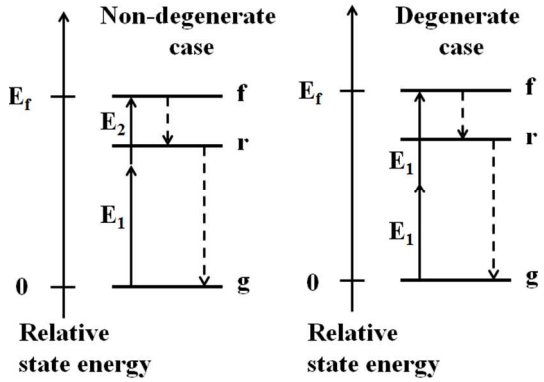

Fig. 1 The principle of TPA.[30]

Two-photon absorption can also be divided into sequential and simultaneous absorption. In sequential absorption, the absorbing species are excited to a real intermediate state, and then a second photon is absorbed. In simultaneous absorption, there is no real intermediate energy state. This process can be considered as an initial interaction of a photon of energy E_1 with the molecule forms a temporary virtual state of energy E_1 above the ground state, which is not a real state of the molecule and it exists only for extremely short time interval (τ_v).[27] If a photon of energy E_2 interacts with the molecule during τ_v, it can be excited to state *f*. The order of magnitude for τ_v estimated from the uncertainty principle is 10^{-15}-10^{-16} s for photon energies in the visible and near-IR ranges.[27] The transition probability for the TPA process depends on the square of the intensity of the laser beam used for the excitation when the two photons have the same energy. If two photons have different energies, the transition probability depends on the product of the intensities of the two laser beams.[29] That characteristic guarantees that TPA absorption only occurs in the focus of laser beam, indicating that the chemical reaction originating from TPA concentrates in the vicinity of the focus region.

In order to realize the full potential of the TPA technology, highly active molecules with large TPA cross section (δ_{TPA}) are desired. δ_{TPA} is widely used as a scale to evaluate TPA activity of a material and its unit is Goeppert-Mayer (GM, 1 GM = 10^{-50} cm^4/photon·molecule). Since 1990s, the research on design and synthesis of new molecules with enhanced δ_{TPA} has been widely carried out. Numerous molecules have been designed and synthesized for investigating the relationship between molecular structures and δ_{TPA}, in order to establish well-defined structure-property relationship with systematically varied molecular structural factors and precisely reproducible characterization of two-photon properties. The detailed knowledge of molecular design parameters of new molecules with enhanced δ_{TPA} has been achieved. Intramolecular charge transfer (ITC) has been proved to be a key factor to determine the δ_{TPA} of molecules. Therefore, much effort of molecular design for enhancing TPA activity has been focused on the improvement of ITC by modifying electronic structures of

molecules through expanding the length of π-conjugated system and introducing strong electronic donor and acceptor groups at the ends of the π-conjugated system.[13, 27, 28]

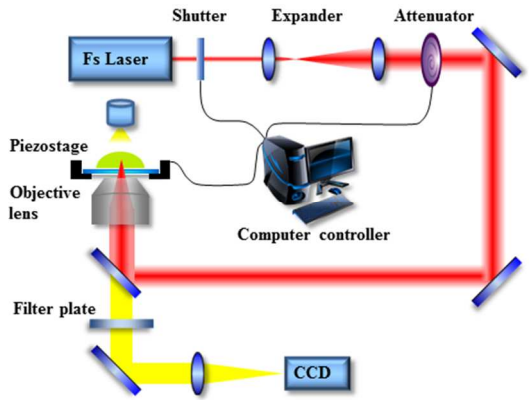

Fig. 2 A typical experimental setup for TPPM in our lab.[31]

TPPM has been the most well-developed TPA-based fabrication technique. In this technique, Ti:Sapphire femtosecond laser with 780-800 nm wavelength is frequently used to drive TPP. Here, the process of TPPM is illustrated by using the experimental setup in our lab (Fig. 2).[31] A near-infrared Ti:sapphire femtosecond laser beam (Tsunami, Spectra-Physics) with a center wavelength of 800 nm, a pulse width of 80 fs, and a repetition rate of 80 MHz is used for TPP. The beam is tightly focused into the photoresist on a glass cover slip with an oil-immersion objective lens (60×, numerical aperture = 1.42). The photoresist is scanned by the focused beam in three dimensions with the xyz-step motorized stage (Physik Instrumente) controlled by a computer. After fabrication, the unpolymerized photoresist is washed out with ethanol and the desired 3D microstructure can be achieved. The photoresists include negative-tone and positive-tone photoresists.[32] For negative photoresists, TPA results in the crosslinking of polymer chains through radical polymerization, making the exposed region insoluble to the developing solvent and the structure is written directly in the sample. On the contrary, for positive photoresists, TPA causes polymeric chains to cleave through photoacid degradation and become soluble to the developing solvent, so the reverse structure is written in the sample.[33] Negative photoresists containing acrylic oligomers or epoxy resins are the most popular photoresists for TPP. Their fundamental ingredients contain photoinitiators used for radical generation, monomers constituting the main skeleton of micro-nanostructures and crosslinkers ensuring the final microstructures to resist to the developing solvents. Resolution as an important parameter for TPPM is mainly controlled by laser power and exposure time, which intensely depend on photoinitiator as an indispensable component of negative resins.

C. Widely used negative photoresist in TPPM

The photoresist used for TPPM is usually a viscous liquid, an amorphous solid, or a gel. The first photoresist used for TPPM is acrylate photopolymer named SCR500, a commercially available resin composed of urethane acrylate monomers and oligomers as well as photoinitiators, which is transparent to an infrared laser and allows it to penetrate deeply. SCR500 can polymerize rapidly with low shrinkage and the microstructures formed are mechanically and chemically stable.[34] Due to versatile chemistry of acrylate photopolymers, they have not only been used in pure form but also doped with other materials to realize some functions. In our previous study, we developed a facile strategy for the in situ synthesis of semiconductor-polymer nanocomposites based on CdS and acrylate photopolymers. Furthermore, we demonstrated multicolor 3D microfabrication of nanocomposites by combining TPPM and the in situ synthesis of semiconductor nanoparticles in a polymer matrix with fine size control.[8]

Besides SCR500, another widely used commercial photoresist in TPPM is SU-8, a negative, epoxy-based materials commonly used for the fabrication of structures with high-aspect ratio. When the laser power reaches the threshold of polymerization, SU-8's long molecular chains begin to crosslink and the final microstructure formed can resist to be developed by the commonly used solvents. SU-8 is thermally stable, transparent in the visible and highly resistant to solvents, acids and bases, which make it suitable for permanent application. SU-8 has been already employed for the fabrication of photonic and microfluidic structures as well as metamaterial covered with metal.[3]

Commercial photoresists named ORMOCERs with an inorganic (-Si-O-Si-) backbone functionalized with organic groups such as acrylates or epoxides has also been widely used in TPPM. ORMOCERs combine properties of silicate glasses such as hardness, chemical and thermal stability, and optical transparency with the laser processing at low temperatures of organic polymers. The organic side chains can crosslink to form a durable, biocompatible solid. Therefore, ORMOCERs are often used as photocurable dental composites.[3, 18]

Photoresists composed of PEG based synthetic monomers and crosslinkers have drawn wide interest because PEG is widely used in tissue engineering and is FDA approved for various medical applications such as cosmetics, lotions and drug formulations. 3D hydrogels fabricated via TPPM are usually based on this kind of negative photoresists.[17-20]

D. Development of TPP initiators

Perry and Marder firstly established a series of effective rules for design of TPP initiators. Their strategies of molecular design of TPP initiators include (1) a chromophoric group with a large δ_{TPA}, such as a D-π-D structure; (2) a chemical functionality that has a high efficiency of initiation, such as those in UV initiators; and (3) a mechanism by which excitation of the chromophore leads to activation of the chemical functionality, such as an electron-transfer process.[13, 35] Recently, Li et al. used classical aldol condensation reactions to synthesize a series of linear and cyclic benzylidene ketone-based TPP initiators containing double bonds and dialkylamino

groups in one step. Systematic investigations of structure-activity relationships were conducted via quantum-chemical calculations and experimental tests, which proved the size of the central ring of TPP initiators significantly affected the TPP initiation efficiency.[36] Even though a series of 2PA active chromophores have been reported, not all of them are unsuitable as photoinitiators due to the fact that fluorescence and radical generation are competitive processes of the excited state deactivation.

Our works focused on design and synthesis of TPP initiators (Fig. 3a, 3b and 3c) with C_{2v} symmetrical structure that have large δ_{TPA} and low fluorescence quantum efficiency.[37-41] Not only large δ_{TPA} but also low fluorescence quantum efficiency contributed to the excellent property of TPP initiators. In our previous study, C_{2v} symmetrical anthraquinone derivatives, 2,7-bis(2-(4-dimethylamino-phenyl)-vinyl)anthraquinone (BDPVA) was synthesized by Wittig reaction. It has low fluorescence quantum yield and large δ_{TPA} of 1635 GM at the wavelength of 800 nm. BDPVA of 0.02 wt% in resin composed of methacrylic acid as monomer and dipentaerythritol hexaacrylate as crosslinker exhibited a low threshold of 3.67 mW at a scanning speed 10 μm s^{-1}.[38] In fact, compared with our subsequent reported TPP initiators, BDPVA even has higher initiating ability, but its solubility in organic solvent and resin is poor, which limits its application in TPP. Like anthraquinone, carbazole is also often used as a conjugation center to prepare TPA compounds. Moreover, carbazole is a highly efficient coinitiator for SPP. Xing et al. designed and synthesized A-π-D-π-A C_{2v}-shaped 3,6-bis(phenylethynyl)carbazole based chromophores as TPP initiators combining a large δ_{TPA} with facilitated radical formation. 9-Benzyl-3,6-bis(4-nitrophenylethynyl)carbazole (BBNC) shows a strong TPA around 800 nm and exhibits very high TPP initiating sensitivity. BBNC of 0.18% molar ratio in resin composed of methacrylic acid and dipentaerythritol hexaacrylate exhibited a low threshold of 0.8 mW at a scanning speed 10 μm s^{-1}. The lowest loading of BBNC in resin is up to 0.012 mol% with a threshold power of 3.2 mW.[39] Besides carbazole, anthracene has been widely used as UV photosensitizers or photoinitiators. Moreover, the good co-planarity of anthracene as an efficient π-center could contribute to the improvement of δ_{TPA}. Xing et al. developed a series of C_{2v} symmetrical TPA compounds with anthracene core. 2,7-Bis[2-(4-dimethylamino-phenyl)vinyl]-9,10-dipentyloxy-anthracene (BPDPA) of 0.18% molar ratio in resin composed of methacrylic acid and dipentaerythritol hexaacrylate exhibited a dramatically low threshold of 0.64 mW at a scanning speed of 10 μm s^{-1}. Moreover, the threshold of BPDPA was only increased to 2.53 mW at a scanning speed of 1000 μm s^{-1}.[41] High TPP initiating sensitivity of our designed photoinitiators results from their large δ_{TPA} and low fluorescence yield. Our proposed concept of molecular design provides good prospects for developing TPP initiators with high initiating efficiency.

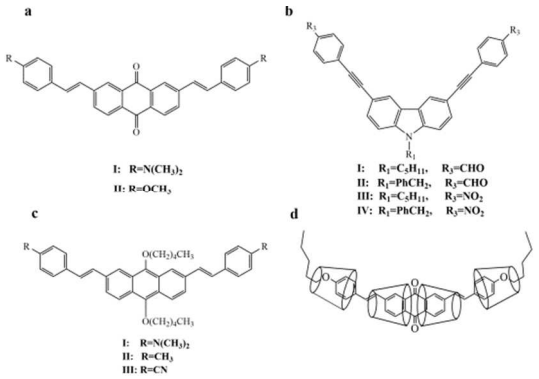

Fig. 3 TPP initiators developed in our lab.

At present, most of TPP initiators are hydrophobic, which is adverse for fabrication of 3D hydrogels due to the residue of organic solvent used to prepare the photoresist. Besides the desired high yield of radical generation, TPP photoinitiators should not affect the biological environment for a biomedical application. The ideal structures should be highly hydrophilic and noncytotoxic, and these aspects have been considered while developing the 2PP photoinitiators. Several groups developed water soluble TPP initiators to fabricate 3D hydrogels in aqueous medium, but the laser power for fabrication was as high as to tens of mW.[42, 43] Therefore, the absence of TPP initiators with high efficiency in aqueous medium is still the crucial barrier for TPP microfabrication of 3D hydrogels. To address that issue, we provided a universal method to prepare water soluble TPP initiator with high efficiency by using host-guest chemical interaction.[31] In detail, we firstly synthesized a novel TPP initiator, hydrophobic 2,7-bis(2-(4-pentaneoxy-phenyl)-vinyl)anthraquinone (BPPVA) with a C_{2v} symmetrical structure through Wittig reaction. The long alkyl chain can guarantee the excellent solubility of BPPVA in organic solvents to assemble with 2-hydroxypropyl-β-cyclodextrins (2-Hp-β-CDs) effectively. A water soluble TPP initiator (WI) (Fig. 3d) was then prepared by combining BPPVA and 2-Hp-β-CDs through host-guest chemical interaction. In aqueous medium, WI showed a δ_{TPA} of around 200 GM at the wavelength of 780 nm which was much higher compared with those of commercial initiators. The threshold energy of TPP for the resin with WI as a photoinitiator (the molar ratio of BPPVA in resin is 0.03%) was 8.6 mW. Compared other groups' works, the laser threshold energy for fabrication of 3D hydrogels was dramatically decreased and the resolution was largely improved.

E. Improvement of TPP resolution

The milestone for TPP resolution breakthrough was Kawata's report in Nature in 2001.[14] Kawata et al. fabricated 10 μm-long and 7 μm-high bulls that are the smallest model animals ever made artificially, and are about the size of a red blood cell (Fig. 4). The tiny volume of such micromachines would allow them to be transported in the human body even through the smallest blood vessels, for example to deliver clinical treatments. In this work, Kawata et al. improved the resolution to 120 nm beyond

the optical diffraction limit and elaborated the precise mechanism, indicating that high resolution was attributed to the threshold of TPP. Due to the quadratic dependence of TPA probability on the photon fluence density, polymerization occurs only in the vicinity of the focal spot and the size of solidified voxels (3D volume elements) is limited. Furthermore, photogenerated radicals in this volume are subject to scavenging by dissolved oxygen molecules, so polymerization reactions are not initiated and propagated if the exposure energy is less than a critical value defined as the threshold of TPP. In this case, the optical diffraction limit imposed by Rayleigh criteria is simply a measure of focal-spot size, and has no real restraint on the actual size of solidified voxels. Therefore, voxels of any small size can be achieved by choosing an appropriate laser-pulse energy and exposure time, because only the region with energy above the TPP threshold is polymerized. This work illustrates the mechanism behind the high TPP resolution, indicating that the threshold is the crucial factor to determine the TPP resolution, which tells us that the TPP resolution can be further improved by lowering the threshold.

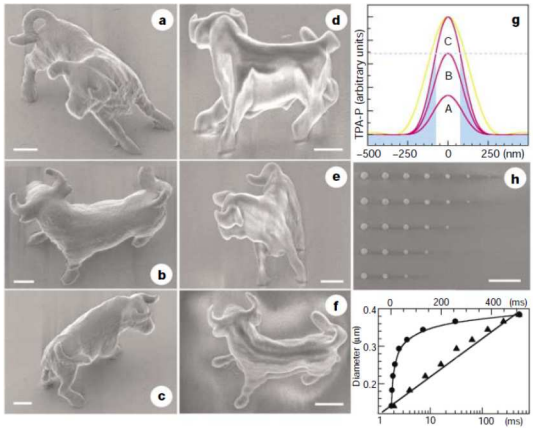

Fig. 4 a-c, Bull sculpture produced by TPP through raster scanning; the process took 180 min. d-f, Bull sculpture produced by combining common SL and TPP; the process took 13 min. g, Achievement of subdiffraction-limit resolution, where A, B and C respectively denote the laser-pulse energy below, at and above the TPP threshold (dashed line). The yellow line represents the range of single-photon absorption. h, Scanning electron micrograph of voxels formed at different exposure times and laser-pulse energies. i, Dependence of lateral spatial resolution on exposure time.[14]

Takada et al. developed a method based on trade-off of quencher diffusion and radical generation to improve the resolution of TPP to 100 nm.[21] This method combined a mobile quenching molecule with a slow laser scanning speed to allow the diffusion of the quencher in the scanned area and the depletion of the generated radicals. However, the addition of radical quenchers could result in an increase of threshold for TPP. Moreover, the voxel-size reduction by adding radical quenchers causes the low mechanical strength of a polymerized structure due to its low molecular weight, because the mechanical strength of polymers depends on the length of polymerized chains. In this case, a microstructure with a low mechanical strength is easily distorted by the surface tension of a rinsing material in the developing process.[4]

In our previous work, Xing et al. improved lateral spatial resolution (LSR) of TPP to 80 nm (Fig. 5), the tenth of the laser beam with a central wavelength of 800 nm, by using an anthracene derivative (9,10-bis-pentyloxy-2,7-bis[2-(4-dimethylamino-phenyl)-vinyl]anthracene (BPDPA) as a highly sensitive and efficient photoinitiator, which contributes to a low threshold and short exposure time.[22] Furthermore, we demonstrated that TPP resolution is proportional to the efficiency of initiator, indicating that the LSR could be improved using more sensitive initiators in the future. In another work, we investigated the phenomena affecting LSR and aspect ratio (AR) in TPP. A LSR of 50 nm and an AR of 1.38 have been achieved for photocured polymer lines on the surface of a substrate by continuing scanning mode. Theoretical analysis based on the distribution of light intensity in this setup indicates that the LSR could be improved to better than 20 nm.[44] This work indicates that the asymmetric shrinkage of voxel in the axial and lateral directions has a significant impact for obtaining features of low AR, which are a critical requirement for construction of micro/nanodevices by TPPM.

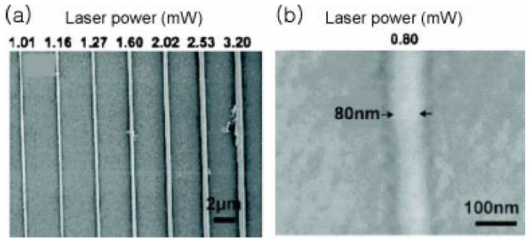

Fig. 5 Scanning electronic microscopy (SEM) images of (a) a pattern fabricated by using different laser powers from 1.01 mW to 3.20 mW at a linear scan speed of 50 μm/s. (b) Magnified SEM image of the polymer line (80 nm) fabricated by using a laser power of 0.80 mW and a linear scan speed of 50 μm/s.[22]

The repolymerization technique has been developed to reduce the feature size in the TPP. TPP regions can be divided into three different parts, including (1) a fully polymerized region with high molecular weight and degree of crosslinking (hard solid state), (2) a weakly polymerized region with low molecular weight and degree of crosslinking (soft solid state), and (3) an unpolymerized region (liquid state). Generally, region (3) is removed by rinsing materials in the developing process. Region (2) is possible to reserve after development if molecular weight and degree of crosslinking are suitable in this region. This character for the repolymerization technique can be utilized to reduce the feature size in the TPP. The feature size of TPP using SCR500 resin was reduced to sub-25-nm at high scan speed of laser focus and laser power by controlling the distance between two closed structures to fabricate the suspended lines (Fig. 6a). The feature sizes were dependent not only on the laser power and the laser focus scan speed but also on the surrounding existing structures. When two polymerized structures became close enough, lines along the perpendicular direction of them with feature size of sub-20-nm (Fig. 5b) were formed by repolymerization of the low-degree polymerized

zone, which can be used to fabricate structures such like microchannels including nanofibers (Fig. 5c) with ultrasmall feature sizes for TPP microfabrication.[24] Although The repolymerization technique provided a useful method to improve the resolution of TPP, it is difficult to fabricate complex microstructures.

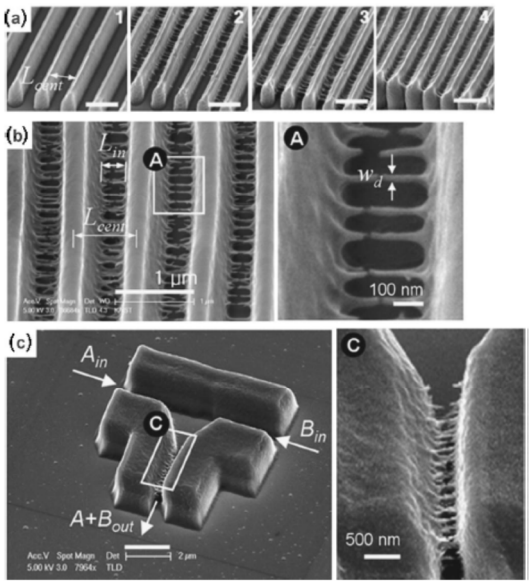

Fig. 6 (a) SEM images of fabricated nanofibers with varying central distance (L_{cent}): (1) 900, (2) 770, (3) 670, and (4) 620 nm, respectively. The scale bars are 1 μm. (b) Well-fabricated nanofibers among the densely polymerized line patterns. The distance between lines (L_{in}) is approximately 270 nm, and the diameters of the nanofibers are 20-30 nm. (c) SEM images of fabricated microchannels including nanofibers in their interiors.[24]

Unlike previous strategies from chemical viewpoint, Li et al. developed a novel physical strategy to improve the resolution of TPP. They designed a different 3D printing system of TPP. In detail, they used pulsed 800 nm light to initiate cross-linking in a photoresist and single-photon absorption of continuous-wave 800 nm light simultaneously to deactivate the photopolymerization. By employing spatial phase-shaping of the deactivation beam, they demonstrated the fabrication of features with scalable resolution along the beam axis, down to a 40 nm minimum feature size.[45] If this method is combined with usage of TPP initiators with high efficiency, TPP resolution will be further improved.

Since 3D hydrogels easily deform due to the high water content, the improvement of their spatial resolution faces a big challenge. All typical works described above provided many useful methods to improve the resolution of 3D hydrogels. Undoubtedly, it is a convenient and direct method to use highly sensitive initiator to improve the resolution of 3D hydrogels fabricated by TPP microfabrication. Recently, we used a water-soluble initiator (WI) with high efficiency to initiate radical polymerization to fabricate 3D hydrogels and LSR of the polymer line reached to around 200 nm (Fig. 7c).[31] It can be anticipated that the resolution of 3D hydrogels will be further improved with more sensitive TPP initiator in future.

F. 3D hydrogels fabricated via TPP

Hydrogels are commonly referred to as polymeric materials with water contents similar to that of soft tissues. Hydrogels have been widely used in tissue engineering and drug delivery.[17-19] Precise 3D configuration for hydrogels is crucial for those biomedical applications.[20] Contrary to other lithographic techniques lack of the ability to precisely control 3D morphology of microstructures fabricated, TPP is an advanced 3D printing technology to fabricate 3D hydrogels with precise 3D configuration. Watanabe et al. fabricated a photoresponsive 3D hydrogel of cantilever that defects under illumination.[45] The hydrogel was prepared from a comonomer solution containing acryloylacetone, acrylamide and N,N'-methylene bisacrylamide. The photoresponse of the cantilever was activated by photoexcitation of acetylacetone groups at 244 nm. Deflection of the cantilever by ~45° was realized upon UV irradiation for 20 min. This work represented a first step toward fabrication of optically controllable and movable 3D micromachine components and microfluidic systems. It was believed that developing higher performance and reversible photoresponsive hydrogels can both expand the applications of TPPM and offer new capabilities in a number of microtechnologies. Ovsianikov et al. reported several different 3D hydrogels used for 3D cell scaffolds.[16, 46] They produced highly porous 3D hydrogel scaffolds by TPP of poly(ethylene glycol) diacrylate (PEGda) with a molecular weight of 742 Da and seeded them with cells by means of laser-induced forward transfer (LIFT). With TPP technique multiple cell types can be printed into 3D scaffolds. Combination of LIFT and TPP provides a route for the realization of 3D multicellular tissue constructs and artificial ECM engineered on the microscale.[16] Torgersen et al. prepared 3D hydrogels as a toolbox for mimicking the extracellular matrix.[47] Using a highly efficient water-soluble initiator, 1,4-bis(4-(N,N-bis(6-(N,N,N-trimethylammonium)hexyl)amino)-styryl)-2,5-dimethoxybenzene tetraiodide, photocurable resin composed of 700 Da PEGda was processed with high precision and reproducibility at a writing speed of 10 mm/s. The biocompatibility of the applied materials was verified using caenorhabditis elegans as living test organisms. Furthermore, these living organisms were successfully embedded within a 200 × 200 × 35 μm^3 hydrogel scaffold. This work proved that TPPM can be used to polymerize poly(ethylene glycol)-based materials into three-dimensional structures with precisely defined geometries that mimic the physical and biological properties of native cell environments.

In our previous work, Xiong et al. used an asymmetric TPP microfabrication method to fabricate the size- and shape-controlled stimuli-responsive asymmetric hydrogel microcantilevers. Photopolymerisable gel precursor was prepared by dissolving monomer acrylamide, co-monomer 2-acrylamido-2-methylpropane sulfonic acid sodium, crosslinker N,N'-methylene bis(acrylamide), as well as photoinitiator benzil and photosensitizer 2-benyl-2-(dimethylamino)-4'-morpholinobutyrophenone into the mixed hydrophilic solvents

consisted of methanol, DMSO and glycerol. The reversible ion-responsive hydrogel microcantilevers exhibit attractive and controllable bending behavior due to their asymmetric deformation to external ions.[48] This 3D stimuli-responsive hydrogels were promising for the application of microactuators and micromanipulators. This designable TPPM technique and the stimuli-responsive behavior of asymmetric microstructure of hydrogel with versatility in the shape would be prospective for developing biomedical microdevices. In another work, Xing et al. fabricated 3D hydrogels of woodpile structure similar to cell scaffolds (Fig. 7) with 700 Da PEGda as monomer and crosslinker by using an average power of 9.7 mW and a scanning speed of 30 μm s^{-1}.[31] The laser threshold energy for fabrication of 3D hydrogels was dramatically decreased and the resolution was largely improved. This work provides a green and facile method to fabricate 3D hydrogels via TPPM in aqueous medium.

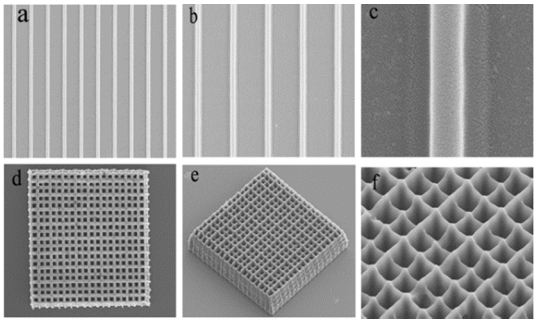

Fig. 7 The SEM images on TPPM. (A-C) show the solid polymer lines and (D-F) show 3D hydrogels with a woodpile structure with 80 × 80 × 17 μm^3.[31]

Although commercially available PEGda has been widely used to fabricate 3D hydrogel due to its high reactivity and tunable physical properties, the interaction between cells and PEGda is known to be rather weak and there is required for new hydrophilic monomers/oligomers to improve the bioactivity of the formed scaffolds. Monomers/oligomers derived from natural polymers, especially from those that are components of the native extracellular matrix, are prior to be considered. Hyaluronic acid (HA) is a chief component of human extracellular matrix (ECM), representing an extremely attractive starting material for the fabrication of 3D hydrogel scaffolds for tissue engineering. However, mechanical properties of HA are poor. Kufelt et al. combined HA and PEGda to prepare 3D hydrogel scaffolds for bone tissue engineering. In detail, HA was combined and covalently cross-linked with PEGda in situ. TPP was applied for the fabrication of well elaborated 3D HA and HA-PEGda scaffolds with different geometries and pore sizes.[49] Such structures provided promising prospects for cell investigations in a reproducible 3D organized hydrogel milieu.

This ability to spatially fabricate the precise structure of vascular network is crucial for tissue engineering. In order to generate highly complex, three-dimensional, and biologically relevant micropatterned materials such like vascular network, Culver et al. have developed a process that utilizes confocal images from tissues to guide two-photon laser scanning lithography (TP-LSL) patterning of biomolecules immobilized to hydrogel scaffolds.[50] The principle and the process of this method were shown in Fig. 8. Confocal microscopy was used to image labeled tissues in three dimentional. Each optical section was then processed to reconstruct the cross-sectional structure of the tissue using a mosaic of regions of interest (ROIs). Next, these ROIs were used to control precise scanning of a laser scanning microscope. To pattern a 3D structure, a mosaic of ROIs for each axial cross section was utilized to sequentially pattern each corresponding plane of the hydrogel. 3D hydrogels of imaged vasculature from the retina, cerebral cortex, and heart were fabricated by TPP of PEG-PQ, which has been rendered biodegradable through the incorporation of a matrix metalloproteinase-sensitive peptide (GGPQGIWGQGK, abbreviated PQ) into the backbone of a PEG-diacrylate derivative. This method can be employed to engineer biomaterials to recreate essential elements of endogenous cellular microenvironments and recapitulate tissue structures.

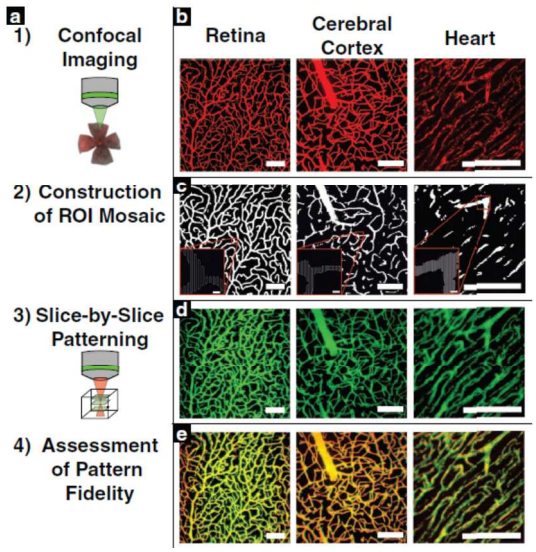

Fig. 8 The principle and process of TP-LSL.[50]

Conclusions, challenges and future perspectives

3D printing technology has presented wide applications and infinite potential of development in science and industry. When combined with two-photon polymerization microfabrication (TPPM), a highly precise manufacturing technology, well-defined three-dimensional structures can be obtained. TPPM has achieved many applications in the fields of micro/nanophotonics, micro-electromechanical systems, microfluidics, biomedical implants and microdevices. In particular, TPPM is very useful in tissue engineering and drug delivery due to its powerful fabrication ability of precise microstructures with high spatial resolution not only on the microscopic scale but also on the nanoscale. The fabrication of 3D hydrogels widely used in tissue engineering and drug

delivery has been an important research area of TPP microfabrication.

However, 3D hydrogels fabricated by TPPM are confronted with low spatial resolution, which is adverse to fabricate microstructures with precise control over shape and pore dimensions on the nanoscale. Another issue faced by 3D hydrogels fabricated by TPPM is time consuming, which originates from the characteristic of TPPM and lack of water soluble initiators with high efficiency.

It is known that spatial resolution of TPPM depends on scanning rate and laser power. The two parameters of scanning rate and laser power can be optimised to improve spatial resolution of TPPM by using highly sensitive initiators. To solve the issue of time consuming of TPPM, several strategies can be used. One strategy is the use of microlens array (MLA) in TPPM. The MLA is a collection of small lenses arranged in an array on a transparent substrate. This method is suitable for the fabrication of periodic structures and multi-microfabrications.[26] Scanning route can be optimized to shorten fabrication time through modification of computer procedure controlling the movement of 3D piezostage or galvano mirrors to improve the efficiency of fabrication. High efficient TPP initiators can improve scanning rate and lower laser power, which benefit to enhance the throughput of femtosecond laser processing. In future, intense endeavour needs to be focused on the design and preparation of water soluble TPP initiators with high efficiency. Of course, laser technology is needed to be developed to the rapid increasing demand in basic science research and industrialization.

Acknowledgements

Authors thank the support of the National Natural Science Foundation of China (31371014, 91323301, 61205194 and 61475164) and Tianjin Natural Science Foundation (13JCYBJC16500).

Notes and references

[a]*Department of Polymer Science and Engineering, School of Chemical Engineering and Technology, Tianjin University, Tianjin, 300072, P. R. China. E-mail:* jinfengxing@tju.edu.cn
[b]*Laboratory of Organic NanoPhotonics and Key Laboratory of Functional Crystals and Laser Technology, Technical Institute of Physics and Chemistry, Chinese Academy of Sciences, No.29 Zhongguancun East Road, Beijing 100190, P. R. China.*
[c]*Chongqing Institute of Green and Intelligent Technology, Chinese Academy of Sciences, No.266 Fangzheng Ave, Shuitu technology development zone, Beibei District, Chongqing 400714, P. R. China. E-mail:* xmduan@mail.ipc.ac.cn

1 S. V. Murphy, A. Atala, *Nat. Biotechnol*., 2014, **32**: 773-785.
2 T. A. Campbell, O. S. Ivanova, *Nano Today*, 2013, **8**: 119-120.
3 M. Malinauskas, M. Farsari, A. Piskarskas, S. Juodkazis, *Physics Reports* 2013, **533**: 1-31.
4 S.-H. Park, D.-Y. Yang, K.-S. Lee, *Laser. Photon. Rev*., 2009, **3**: 1-11.
5 S. Wu, J. Serbin, M. Gu, *J. Photochem. Photobiol., A,* 2006, **181**: 1-11.
6 H.-B. Sun, S. Matsuo, H Misawa, 1999, *Appl. Phys. Lett*., 1999, **74**, 786-788.
7 J. Scrimgeour, D. N. Sharp, C. F. Blanford, O. M. Roche, R. G. Denning, A. J. Turberfield, *Adv. Mater*., 2006, **18**, 1557-1560.
8 Z.-B. Sun, X.-Z. Dong, W.-Q.Chen, S. Nakanishi, X.-M.Duan, S. Kawata, *Adv. Mater*., 2008, **20**, 914-919.
9 W. K. Wang, Z. B. Sun, M. L. Zheng, X. Z. Dong, Z. S. Zhao, X.-M. Duan, *J. Phys. Chem. C*, 2011, **115**, 11275-11281.
10 D. Wu, Q.-D. Chen, L.-G. Niu, J.-N. Wang, J. Wang, R. Wang, H. Xia, H.-B. Sun, *Lab. Chip*., 2009, **9**, 2391-2394.
11 P. Tayalia, C. R. Mendonca, T. Baldacchini, D. J. Mooney, E. Mazur, *Adv. Mater*., 2008, **20**, 4494-4498.
12 W. Zhang, P. Soman, K. Meggs, X. Qu, S. Chen, *Adv. Funct. Mater*., 2013, **23**, 3226-3232.
13 B. H. Cumpston, S. P. Ananthavel, S. Barlow, D. L. Dyer, J. E. Ehrlich, L. L. Erskine, A. A. Heikal, S. M. Kuebler, I.Y. Sandy Lee, D. McCord-Maughon, J. Qin, H. Röckel, M. Rumi, X.-L. Wu, S. R. Marder, J. W. Perry, *Nature*, 1999, **398**, 51-54.
14 S. Kawata, H.-B. Sun, T. Tanaka, K. Takada, *Nature*, 2001, **412**, 697-698.
15 A. Ovsianikov, J. Viertl, B. Chichkov, M. Oubaha, B. MacCraith, I. Sakellari, A. Giakoumaki, D. Gray, M. Vamvakaki, M. Farsari, C. Fotakis, *ACS Nano*, 2008, **2**, 2257-2262.
16 A. Ovsianikov, M. Gruene, M. Pflaum, L. Koch, F. Maiorana, M. Wilhelmi, A. Haverich, B. Chichkov, *Biofabrication*, 2010, **2**, 014104.
17 N. A. Peppas, J. Z. Hilt, A. Khademhosseini, R. Langer, *Adv. Mater*., 2006, **18**, 1345-1360.
18 J. Torgersen, X.-H. Qin, Z. Li, A. Ovsianikov, R. Liska, J. Stampfl, *Adv. Funct. Mater*., 2013, **23**, 4542-4554.
19 A. I. Ciuciu, P. J. Cywiński, *RSC. Adv*., 2014, **4**, 45504-45516.
20 M. T. Raimondi, S. M. Eaton, M. M. Nava, M. Laganà, G. Cerullo, R. Osellame, *J. Appl. Biomater. Function. Mater*., 2012, **10**, 56-66.
21 K. Takada, H.-B. Sun, S. Kawata, *Appl. Phys. Lett*., 2005, **86**, 071122.
22 J.-F. Xing, X.-Z. Dong, W.-Q. Chen, X.-M. Duan, N. Takeyasu, T. Tanaka, S. Kawata, *Appl. Phys. Lett*., 2007, **90**, 131106.
23 D. Tan, Y. Li, F. Qi, H. Yang, Q Gong, X.-Z. Dong, X.-M. Duan, *Appl. Phys. Lett*., 2007, **90**, 071106.
24 S. H. Park, T. W. Lim, D.-Y. Yang, N. C. Cho, K.-S. Lee, *Appl. Phys. Lett*., 2006, **89**, 173113.
25 H.-Z. Cao, M.-L. Zheng, X.-Z. Dong, F. Jin, Z.-S. Zhao, X.-M. Duan, *Appl. Phys. Lett*., 2013, **102**, 201108.
26 K.-S. Lee, R. H. Kim, D.-Y. Yang, S. H. Park, *Prog. Polym. Sci.*, 2008, **33**, 631-681.
27 G. S. He, L.-S. Tan, Q. Zheng, P. N. Prasad, *Chem. Rev*., 2008, **108**, 1245-1330.
28 M. Pawlicki, H. A. Collins, R. G. Denning, H. L. Anderson, *Angew. Chem. Int. Ed*., 2009, **48**, 3244-3266.
29 J. Fischer, M. Wegener, *Laser. Photon. Rev*., 2013, **7**: 22-44.
30 M. Rumi, J. W. Perry, *Adv. Opt. Photon.*, 2010, **2**, 451-518.
31 J.-F Xing, J.-H. Liu, T.-B. Zhang, L.-Zhang, M.-L. Zheng, X.-M. Duan, *J. Mater. Chem. B*, 2014, **2**, 4318-4323.
32 Y.-L. Zhang, Q.-D. Chen, H. Xia, H.-B. Sun, *Nano Today*, 2010, **5**, 435-448.
33 M. Farsari, B. N. Chichkov, *Nature. Photon*., 2009, **3**, 450-452.
34 S. Maruo, O. Nakamura, S. Kawata, *Opt. Lett*. 1997, **22**: 132-134.
35 M. Albota, D. Beljonne, J.-L. Brédas, J. E. Ehrlich, J.-Y. Fu, A. A. Heikal, S. E. Hess, T. Kogej, M. D. Levin, S. R. Marder, D. McCord-

Maughon, J. W. Perry, H. Röckel, M. Rumi, G. Subramaniam, W. W. Webb, X.-L Wu, C. Xu, *Science*, 1998, **281**, 1653-1656.

36 Z. Li, N. Pucher, K. Cicha, J. Torgersen, S. C. Ligon, A. Ajami, W. Husinsky, A. Rosspeintner, E. Vauthey, S. Naumov, T. Scherzer, J. Stampfl, R. Liska, *Macromolecules*, 2013, **46**, 352-361.

37 J. Gu, Y. Wang, W.-Q. Chen, X.-Z. Dong, X.-M. Duan, S. Kawata, *New. J. Chem*., 2007, **31**, 63-68.

38 J.-F. Xing, W.-Q. Chen, X.-Z. Dong, T. Tanaka, X.-Y. Fang, X.-M. Duan, S. Kawata, *J. Photochem. Photobiol., A*, 2007, **189**, 398-404.

39 J.-F. Xing, W.-Q. Chen, J. Gu, X.-Z. Dong, N. Takeyasu, T. Tanaka, X.-M. Duan, S. Kawata, *J. Mater. Chem*., 2007, **17**, 1433-1438.

40 W.-E. Lu, X.-Z. Dong, W.-Q. Chen, Z.-S. Zhao, X.-M. Duan, *J. Mater. Chem*., 2011, **21**, 5650-5659.

41 J.-F. Xing, M.-L. Zheng, W.-Q. Chen, X.-Z. Dong, N. Takeyasu, T. Tanaka, Z.-S. Zhao, X.-M. Duan, S. Kawata, *Phys. Chem. Chem. Phys*., 2012, **14**, 15785-15792.

42 S. J. Jhaveri, J. D. Mcmullen, R. Sijbesma, L.-S. Tan, W. Zipfel, C. K. Ober, *Chem. Mater*., 2009, **21**, 2003-2006.

43 T. Watanabe, M. Akiyama, K. Totani, S. M. Kuebler, F. Stallacci, W. Wenseleers, K. Braun, S. R. Marder, J. W. Perry, *Adv. Funct. Mater*., 2002, **12**, 611-614.

44 X.-Z. Dong, Z.-S. Zhao, X.-M. Duan, *Appl. Phys. Lett*., 2008, **92**, 091113.

45 L. Li, R. R. Gattass, E. Gershgoren, H. Hwang, J. T. Fourkas, *Science*, 2009, **324**, 910-913.

46 A. Ovsianikov, M. Malinauskas, S. Schlie, B. Chichkov, S. Gittard, R. Narayan, M. Löbler, K. Sternberg, K.-P. Schmitz, A. Haverich, *Acta. Biomater*., 2011, **7**, 967-974.

47 J. Torgersen, A. Ovsianikov, V. Mironov, N. Pucher, X.-H. Qin, Z.-Q. Li, K. Cicha, T. Machacek, R. Liska, V. Jantsch, J. Stamp, *J. Biomed. Opt*., 2012, **17**, 105008.

48 Z. Xiong, M.-L. Zheng, X.-Z. Dong, W.-Q. Chen, F. Jin, Z.-S. Zhao, X.-M. Duan, *Soft. Matter*., 2011, **7**, 10353-10359.

49 O. Kufelt, A. El-Tamer, C. Sehring, S. Schlie-Wolter, B. N. Chichkov, *Biomacromolecules*, 2014, **15**, 650-659.

50 J. C. Culver, J. C. Hoffmann, R. A. Poché, J. H. Slater, J. L. West, M. E. Dickinson, *Adv. Mater.*, 2012, **24**, 2344-2348.